Tuning Optoelectronic Properties of Double Quantum Dot Structure Using Tight-Binding Model for Photo-Electric Applications

Alaa Ayad K. Al-mebir[1*], Shakir A.A. AL-Saidi[2]

Abstract

In electronics field, researchers and industries have been working to fabricate low-cost optoelectronic devices by using less materials in the fabrication process. Thus, miniaturization concept has been used in the design and synthesis of the fabricated materials and devices based on nano-dimension. However, reducing the used materials would affects the overall performance of the devices and new building blocks materials are needed to pass the performance capacity limits of current silicon-based materials. Quantum Dots DQs have been introduced and attracted much attention among researchers because of their unique characteristics that are necessary for many potential applications by using nano-dimensions structures. These properties include size-tunable optical and other electronic characteristics that are not found in the current bulk materials. Although there has been interested QDs experimental studied that have been already carried out, different theoretical efforts must be introduced in order to provide good understanding of the possible and different QDs applications. In this work, therefore, optoelectronic properties of Double Quantum Dots DQDs system were studied theoretically to provide important information about the possibility of using this system in photoelectric applications. A tight-binding framework was adopted to describe the system, and all the calculations were carried out based on the steady state formalism. The proposed DQD structure was connected to metallic leads and studied to investigate the QD size dependent. The transmission calculation presented first through the electron transport mechanism. Tunneling current and conductance were then presented to provide general understanding about the behavior of the proposed system. A correlation of transmission, current and conductance results with QD radius R, incident photon energy Eph, Temperature and bias voltage have been identified. Therefore, this correlation is strongly supporting the proposal of using DQD system in fabricating nano-scale photovoltaic devices, particularly, solar cells.

Key Words: Steady-State-Formalism, Transmission, Conductance, Current.

DOI Number: 10.14704/nq.2021.19.3.NQ21021 **NeuroQuantology 2021; 19(3):01-10**

Introduction

Semiconductors are solid-state materials with electrical conductivity that lies between insulators and metals conductivities, and it can be tuned by introducing the concept of impurities or doping (Peter & Cardona, 2010). Semiconductors, specifically silicon, have been extensively used to fabricate circuits as well as to form the material foundation for the modern electronics industry due to their electric-field controllable conductivity.

Corresponding author: Alaa Ayad K. Al-mebir
Address: [1*]Department of Physics, College of Education of Pure Sciences, University of Thi-Qar, Nassiriyah, Iraq; Department of Physics and Astronomy, University of Kansas, Lawrence, Kansas, USA; [2]Department of Physics, College of Education of Pure Sciences, University of Thi-Qar, Nassiriyah, Iraq.
[1*]E-mail: alaaayad.eps@utq.edu.iq
[2]E-mail: Shakir.hussain@sci.utq.edu.iq
Relevant conflicts of interest/financial disclosures: The authors declare that the research was conducted in the absence of any commercial or financial relationships that could be construed as a potential conflict of interest.
Received: 20 January 2021 **Accepted:** 24 February 2021

They have been also widely used in optoelectronic devices due to their high response to photo excitation, particularly for light detection and energy conversion (Rudan, 2015).

In electronics field, miniaturization has been considered in the design and synthesis of functional materials and devices based on nano-dimension building blocks.

For instance, the micro-electronics industry has been working on building integrated circuits and storage electronic devices with basic units reaching very small size, down to only few tens of nanometers. However, this variation of the dimension of the devices is very challenging because it affects the device overall performance of photonic circuits (Lodahl, 2017), and brings the current silicon-based electronics to its capability limits (Ito & Okazaki, 2000; Kingon, Maria, & Streiffer, 2000; Lloyd, 2000). Semiconductor materials are the ideal options that can be used to convert energy from the sun because they own a band gap that allows the absorption of incident photons, generation of excited states (excitons), separation of electron-hole pairs, and collecting the resulting charges by electrodes. However, silicon-based semiconductor devices are not ideal for low dimension application due to the loss in the absorption of the active layer. Thus, other semiconductors with higher absorption rate have been introduced to harvest more light in small thickness (Alaa Ayad Khedhair Al-Mebir, 2015).

The concept of semiconductor quantum dots QDs has attracted much attention among studies due to introducing unique characteristics for many potential applications (Lv et al., 2020) by using Nano dimensions materials. These properties include size-tunable optical and electronic characteristics that are not found in the same bulk materials (Jin, Tu, Zhang, & Yan, 2010; Reshma & Mohanan, 2019). Semiconductor quantum dots QDs, like other semiconducting materials, own an intrinsic band gap which allows electrons to pass through by excitation effect generated from incident photon. However, unlike bulk semiconducting materials, QDs have no continuous valence and conduction bands structures that usually exist in macroscopic semiconductors. Instead, QDs have a dislocate electronic structure that is closer to the discrete electronic states usually existed in single atoms. Thus, when the QDs become larger, their band gaps get smaller and their electronic structure becomes more continuous. In other words, the larger the QDs, the closer their band gap to that of the bulk material as explained in Fig. 1. However, unlike in the single atom case, this size-dependence factor allows the band gap energy to be tuned by changing the size of the quantum dot, which provide more options for the fabricating of materials with arbitrary band gap energies (Ciftja, 2013). From what mentioned, the energy gap of QDs can be written as the energy gap of the bulk semiconductor plus the confinement energy of both electrons and holes as follows:

$$E_g(QDs) = E_g(bulk) + \frac{h^2}{8R^2}\left(\frac{1}{m_e{}^*} + \frac{1}{m_h{}^*}\right) \quad (1)$$

where $E_g(bulk)$ is the energy gap of the bulk, h is the Planck's constant, R is the radius of the QDs, $m_e{}^*$ is the effective mass of electron and $m_h{}^*$ is the effective mass of hole (Brus, 1984). The uniqueness of QDs beside their tunable band gap is their high absorption of light which is essential in generating photocurrent (Brus, 1984; Ciftja, 2013; H. Sargent, 2005). Further, QDs also have a large quantum yield, which means that their percentage level of absorbed photons is higher than that of emitted photons, that is highly desirable for optoelectronic and solar cells applications (Dabbousi et al., 1997; Lhuillier et al., 2016; Qiao et al., 2016; Song & Yang, 2012). Beside different semiconductor types, semiconductor based on quantum dots QDs have been under study extensively due to their promising optoelectronic properties (Alivisatos, 1996; Bradshaw, Knowles, McDowall, & Gamelin, 2015; Carey et al., 2015; Currie, Mapel, Heidel, Goffri, & Baldo, 2008; Ghosh Chaudhuri & Paria, 2012; Kamat, 2008; McDonald et al., 2005; Nozik et al., 2010; Talapin, Lee, Kovalenko, & Shevchenko, 2010; Walter et al., 2010).

In this work, a DQD structure is introduced which consist of two layers of QDs placed on top of each other. The system also connected to external conductors using two proposed leads. A theoretical study of optoelectronic properties of this DQDs structure have been presented using a tight-binding model to represent the system, and the steady state formalism to obtain all the calculations. Quantum tunneling concept was used in this system by considering the phenomena of electron transfer and tunneling transmission in QDQs. The key challenges for energy applications that has been addressed in this work are tunable

band gap with different QDs sizes and structures; and tuning the photo induced charge transfer processes in QDs, to prepare these QDs for optoelectronic devices especially solar cell devices. Tunneling current of the system resulted from the transmission calculation and its correlation with different parameters was discussed. Further, the conductance of the system shows clear enhancement and response to different parameters including the energy of the incident photons of the system. The presented numerical results provide possible optimization of transmission, current and conductance characteristics which support the basic features of optoelectronic for designing possible nano scale solar cell.

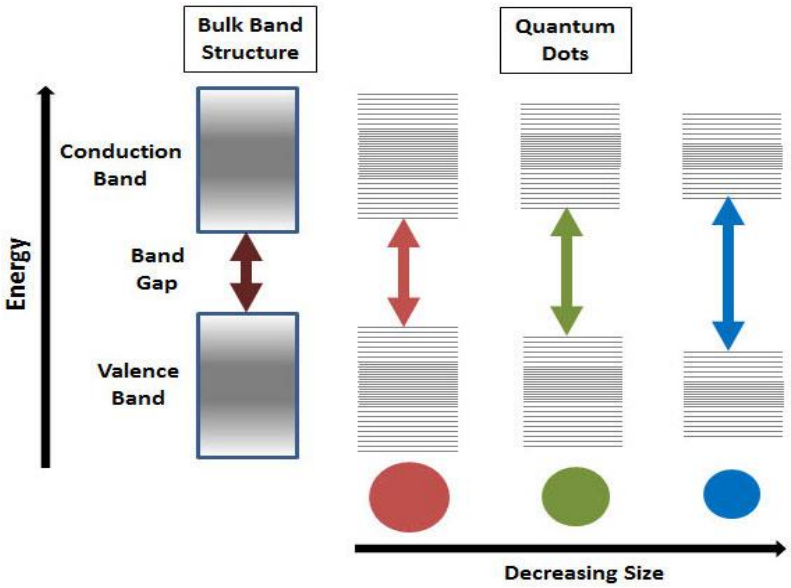

Figure 1. The electronic structure of QD varies with the size of the dot (Ciftja, 2013).

Method and Theoretical Formulation

In this section, the used research method and the theoretical derivations adopted in this work will be presented. The tight-binding model was used in which it was assumed that the DQD system can be described by a chain model, in which an effective energy level of each QD and an effective coupling parameter between any DQD are considered as shown in Fig. 2.

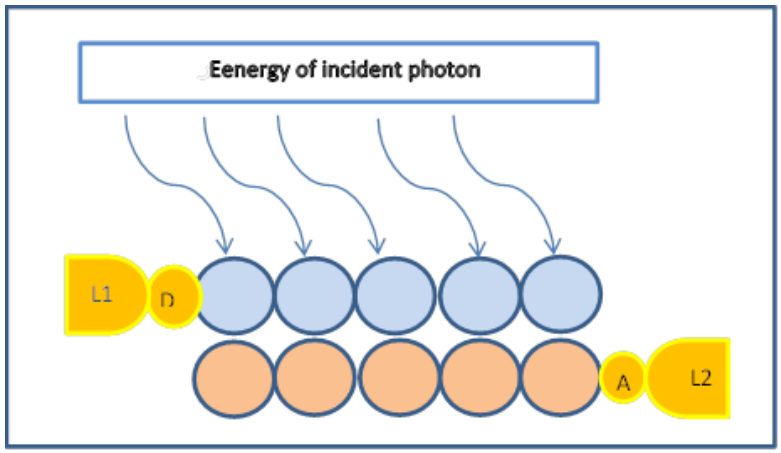

Figure 2. Effect energy of incident photon on the double quantum dots DQD regime.

The eigenvalues of the QDs are calculated by using tight binding model (Alaa Ayad K Al-mebir & Al-Saidi, 2020; Al-Saidi & Al-mebir, 2020; Cuniberti, Maciá, Rodriguez, & Römer, 2007) as can be

represented by the following mathematical expression:

$$E_j = E_Q - 2V_{mn}\cos\left(\frac{\pi j}{N+1}\right) \mp t_{12}, \qquad (2)$$

where E_Q is the energy level of the QD. V_{mn} is the coupling interaction between nearest-neighbor QDs. N represents the total number of the QDs.

In order to represent the proposed system mathematically, a connection between the physics phenomena and math expressions was used based on the quantum principles. Since the simplest tight binding model of the DQD can be considered as a one-dimensional model, every connection between sites reflects the existence of a coupling interaction. The description of DQD as a single site represents a simplification of wire model (AL-Saidi & Al-mebir, 2018). Therefore, the system under consideration that mentioned in Fig. 1 can be represented using the time-independent Hamiltonian and Dirac's notations. This Hamiltonian that represents all the sub-systems interactions can be written as follows:

$$\begin{aligned} H = {} & E_D|D\rangle\langle D| + E_A|A\rangle\langle A| \\ & + \sum_{k_{bs}} E_{k_{bs}}|k_{bs}\rangle\langle k_{bs}| \\ & + \sum_{k_{bb}} E_{k_{bb}}|k_{bb}\rangle\langle k_{bb}| \\ & + \sum_{k_{bs}} [(V_{Ak_{bs}}|A\rangle\langle k_{bs}| + h.c)] \\ & + \sum_{k_{bb}} (V_{Dk_{bb}}|D\rangle\langle k_{bb}| + h.c)] \\ & + \sum_{k_L} (V_{Dk_{L1}}|D\rangle\langle k_{L1}| + h.c \\ & + \sum_{k_R} (V_{Ak_{L2}}|A\rangle\langle k_{L2}| + h.c) \quad (3) \end{aligned}$$

where the indexes D, A, $L1$, $L2$, bs and bb refer to the donor, acceptor, first lead, second lead, lower QDs and upper QDs with total number N. Also, the index k_i refers to the energy wave vector, where i represents the indexes D, A, $L1$, $L2$, bs and bb. E_i refers to the energy level position, and $|i\rangle$ and $\langle i|$ represent the *ket* and *bra* states. V_{ij} refers to the coupling interaction between the subsystems i and j. The wave function of the system can be written as:

$$\begin{aligned} \psi(t) = {} & C_D(t)|D\rangle + C_A(t)|A\rangle + \sum_{k_{bb}} C_{k_{bb}}(t)|k_{bb}\rangle \\ & + \sum_{k_{bs}} C_{k_{bs}}(t)|k_{bs}\rangle + \sum_{k_{L1}} C_{k_{L1}}(t)|k_{L1}\rangle \\ & + \sum_{k_{L2}} C_{k_{L2}}(t)|k_{L2}\rangle, \end{aligned}$$

where $C_i(t)$ refers to the linear expansion coefficients. The equations of motion for $C_i(t)$ can be obtained by using time-dependent Schrodinger equation given by:

$$\frac{\partial\psi(t)}{\partial t} = -iH\psi(t) \qquad (5)$$

Thus, the following set of related equations can be obtained:

$$\begin{aligned} \dot{C}_D(t) = {} & -iE_D C_D(t) - i\sum_{k_{bb}} V_{Dk_{bb}} C_{k_{bb}}(t) \\ & - i\sum_{k_{L1}} V_{Dk_{L1}} C_{k_{L1}}(t) \quad (6) \end{aligned}$$

$$\begin{aligned} \dot{C}_A(t) = {} & -iE_A C_A(t) - i\sum_{k_{bs}} V_{Ak_{bs}} C_{k_{bs}}(t) \\ & - i\sum_{k_{L2}} V_{Ak_{L2}} C_{k_{L2}}(t) \quad (7) \end{aligned}$$

$$\dot{C}_{k_{bb}}(t) = -iE_{k_{bb}} C_{k_{bb}}(t) - iV_{k_{bb}D} C_D(t) \quad (8)$$

$$\dot{C}_{k_{bs}}(t) = -iE_{k_{bs}} C_{k_{bs}}(t) - iV_{k_{bs}A} C_A(t) \quad (9)$$

$$\dot{C}_{k_{L1}}(t) = -iE_{k_{L1}} C_{k_{L1}}(t) - iV_{k_{L1}D} C_D(t) \quad (10)$$

$$\dot{C}_{k_{L2}}(t) = -iE_{k_{L2}} C_{k_{L2}}(t) - iV_{k_{L2}A} C_A(t) \quad (11)$$

where, $V_{ij} = V_{ji}$ and i, j=A, D, k_{L1}, k_{L2}, k_{bs} and k_{bb}.

By using condition stationary states, we define $C_j(t)$ as $C_j(t) = \bar{C}_j e^{-iEt}$ where E represents the types of system eigenvalues. By setting $\dot{\bar{C}}_j = 0$, and following the separation methods, the following can be written:

$$V_{k_i\alpha} = v_{ki} V^{I\alpha} \qquad (12)$$

$$\overline{C}_{ki} = v_{ki}\bar{\bar{C}}_I \qquad (13)$$

where I=A, D, L1, L2, bs and bb and α=A, D, L1, L2, bs and bb.

By substituting these definitions in Eqs. (7)-(11), we can get:

$$\bar{C}_A(E) = \frac{1}{E - E_A}\left\{ V^{AL2}\sum_{k_{L2}} |v_{k_{L2}}|^2 \bar{\bar{C}}_{L2} + V^{Abs}\sum_{k_{bs}} |v_{k_{bs}}|^2 \bar{\bar{C}}_{bs} \right\} \qquad (14)$$

$$\bar{\mathrm{C}}_D(\mathrm{E}) = \frac{1}{\mathrm{E}-\mathrm{E}_\mathrm{D}}\left\{V^{DL1}\sum_{k_{L1}}\left|v_{k_{L1}}\right|^2\bar{\bar{C}}_{L1} + V^{Dbb}\sum_{k_{bb}}\left|v_{k_{bb}}\right|^2\bar{\bar{C}}_{bb}\right\} \quad (15)$$

$$\bar{\bar{\mathrm{C}}}_{\mathrm{bb}}(\mathrm{E}) = \frac{1}{\mathrm{E}-\mathrm{E}_{\mathrm{bb}}}\{V^{bbD}\bar{C}_D\} \quad (16)$$

$$\bar{\bar{\mathrm{C}}}_{\mathrm{bs}}(\mathrm{E}) = \frac{1}{\mathrm{E}-\mathrm{E}_{\mathrm{bs}}}\{V^{bsA}\bar{C}_A\} \quad (17)$$

$$\bar{\bar{\mathrm{C}}}_{\mathrm{L1}}(\mathrm{E}) = \frac{1}{\mathrm{E}-\mathrm{E}_{\mathrm{L1}}}\{V^{L1D}\bar{C}_D\} \quad (18)$$

$$\bar{\bar{\mathrm{C}}}_{\mathrm{L2}}(\mathrm{E}) = \frac{1}{\mathrm{E}-\mathrm{E}_{\mathrm{L2}}}\{V^{L2A}\bar{C}_A\} \quad (19)$$

Then by substituting equations (17) and (19) into (14), the following relations can be obtained:

$$\bar{\mathrm{C}}_{\mathrm{A}}(\mathrm{E}) = \frac{1}{\mathrm{E}-\mathrm{E}_\mathrm{A}-\sum_{AL2}(E)-\sum_{Abs}(E)} \quad (20)$$

Also, by substituting equations (16) and (18) into (15) we can obtain:

$$\bar{\mathrm{C}}_D(\mathrm{E}) = \frac{1}{\mathrm{E}-\mathrm{E}_\mathrm{D}-\sum_{DL1}(E)-\sum_{Dbb}(E)} \quad (21)$$

$$\frac{\bar{C}_A(E)}{\bar{C}_D(E)} = \frac{X_1(E)}{X_2(E)} = \frac{\mathrm{E}-\mathrm{E}_\mathrm{D}-\sum_{DL1}(E)-\sum_{Dbb}(E)}{\mathrm{E}-\mathrm{E}_\mathrm{A}-\sum_{AL2}(E)-\sum_{Abs}(E)} \quad (22)$$

where,

$$X_1(E) = \mathrm{E}-\mathrm{E}_\mathrm{D}-\sum\nolimits_{DL1}(E)-\sum\nolimits_{Dbb}(E) \quad (23)$$

$$X_2(E) = E - E_A - \sum\nolimits_{AL2}(E) - \sum\nolimits_{Abs}(\mathrm{E}) \quad (24)$$

Here $\sum_{Ai}(E) = -i\Delta_{Ai}(E) + \Lambda_{Ai}(E)$, where $\Delta_{Ai}(E)$ represents the broadening function, while $\Lambda_{Ai}(E)$ refers to the quantum shift function, with $i = L1, L2, bb\ and\ bs$. Therefore, the transmission amplitude and the transmission probability can be defined respectively by the following two equations:

$$t(E) = \frac{\bar{C}_A(E)}{\bar{C}_D(E)} \quad (25)$$

and

$$T(E) = |t(E)|^2 \quad (26)$$

Landauer transport formula can be used to calculate the steady state electric current through the active region which is given by (Li & Yan, 2001):

$$I = \frac{2e}{h}\int_{-\infty}^{\infty} T(E)[f_{L1}(E) - f_{L2}(E)]dE \quad (27)$$

Form the transmission probability described in the previous equation, we can obtain the conductance in our model calculation, which can be given by the following formula (Galperin, Ratner, & Nitzan, 2004):

$$G = \frac{2e^2}{h}\int_{-\infty}^{\infty} dE\ T(E)\frac{\partial f_\alpha(E)}{\partial E} \quad (28)$$

where $f_\alpha(E) = \{1 + \exp[E - \mu_\alpha/k_B T_\alpha]\}^{-1}$ is Fermi distribution function of electrons in the lead $\alpha = L1, L2$. μ_α is the chemical potential of the lead α, where $\mu_{L1} = -V/2$ and $\mu_{L2} = +V/2$ and V is the bias voltage. Also, T_α is the temperature of the lead α, in which we used T_{L1}=T_{L2}=T fixed at 300 K, which means that the leads are in thermal equilibrium.

Results and Discussion

In the following sections, optoelectronic characteristics of DQDs system will be presented. This includes transmission probability properties which will include studying the correlation with the incident photons on the system. Also, tunneling current behavior of the system will be presented including studying the relationships between and tunneling current and different other parameters such as QDs radius, incident photon energy, the temperature of the system, and the bias applied voltage. Further, conductance characteristics of the DQDs system will then be explained including the possible correlation with QDs radius, incident photon energy, and the temperature of the system.

Before discussing the results obtained in the presented calculations, we will first mention the values of different parameters used in this numerical computation. These Parameters are taken as following: t_{bs}=-0.1, t_{bb}=-0.1, v_{abs}=- 0.7, v_{dbb} =-0.1 and t_{12}=-0.1 all are in eV unit. The equilibrium Fermi energy E_F is taken as zero. The energy levels of the up and down QDs are -0.045 eV and -0.044 eV, respectively. It should be mentioned that all the calculations carried out using a designed MATLAB code and all figures are plotted using Origin software.

Transmission Probability Results

The transmission probability, also known as tunneling probability in quantum, is well defined to be the ratio of the transmitted intensity to the incident one. It gives very essential understanding about the ability of the material under study to pass the tunneling electrons and can be very useful in tunning overall device performance. For the proposed system and based on eqs. (25 and 26), the transmission probability results as a function of energy for double quantum dots DQD obtained as illustrated in Figs. 3 (a and b) for the case without incident photons and with incident photons, respectively. The peak-dip transmission number is N-1 due to the contribution of the quantum interference effects. These figures show that the transmission peaks become higher with the increase of energy in both cases. Although the curve shapes are identical in both cases, however these is a clear difference in the resonance's positions on the energy axis. The transmission curve of the DQD system with incident photon energy shown in Fig. 3b is shifted to the right side toward the higher energies due to the quantum shift resulted from the additional energy came from incident photons energy. This shows that the DQD system can be sensitive to the incident photons and its response can be recorded to be useful in many optoelectrical applications.

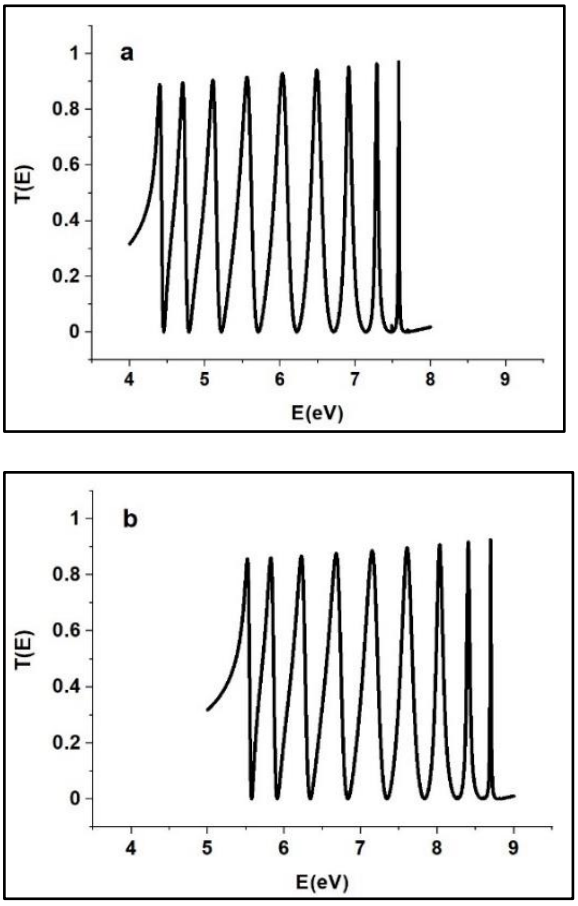

Figure 3. Transmission probability as a function of energy for double quantum dots DQD without incident photons (a) and with incident photons (b).

Tunneling Current Results

The quantum tunneling effect is very common in many semiconductor applications such as electronic circuit, nano-dimension integrated circuits and photovoltaic devices. Since QDs are nano-dimension building blocks of semiconductor devices, they can utilize a quantum tunneling effect represented by the resonant tunneling, tunneling current, of electrons through their potential barriers. Thus, for our proposed QDQs system, the tunneling current was obtained based on eq. (27). The results clearly show a nonlinear dependence of QD radius R, photon energy E_{Ph}, Temperature and bias voltage as shown in Fig. 4 (a, b, c, and d)

respectively. It can be seen in Fig. 4a and 4b that the current was increased sharply in response to specific values of R or E_{Ph} while stayed near the zero at other values. This can be due to the parity between QDs energy gap and incident photon energy. It should be mentioned that it is well known in QDs that the energy gap changes with the change of radius R. Fig. 4c illustrates a clear current – temperature correlation at relatively high temperatures. This can be attributed to the increase in the hybridization between the energy levels of the active region and the left and right leads levels when the temperature increases. At T > 225 K. It can be noticed that the current was enhanced drastically. This can be due to the hopping transport process that occurs between the chemical potentials and active region energy levels located above the chemical potential and between adjacent sites.

Also, the I-V characteristics of the system can provide interested electronic behaviors. Thus, it has been calculated for the current DQDs system as shown in Fig. 4d. It can be found from the I-V characteristics relation that the current-voltage typical relation is applied in which the current is vanished for certain range of bias voltage and started to increase drastically at relatively higher bias voltages. Further, I-V curve show that the relation is approximately symmetric with respect to the absolute value of the bias polarity. This is attributed to the fact that the active region is located at the middle of the gap between the electrodes. The presented results have a good qualitative agreement with the transmission spectrum in the system electronic structure along the zero-current part of the I-V curves. Further, the observed voltage gap in the I–V characteristics cannot be directly attributed to the HOMO-LUMO gap of the proposed DQDs system.

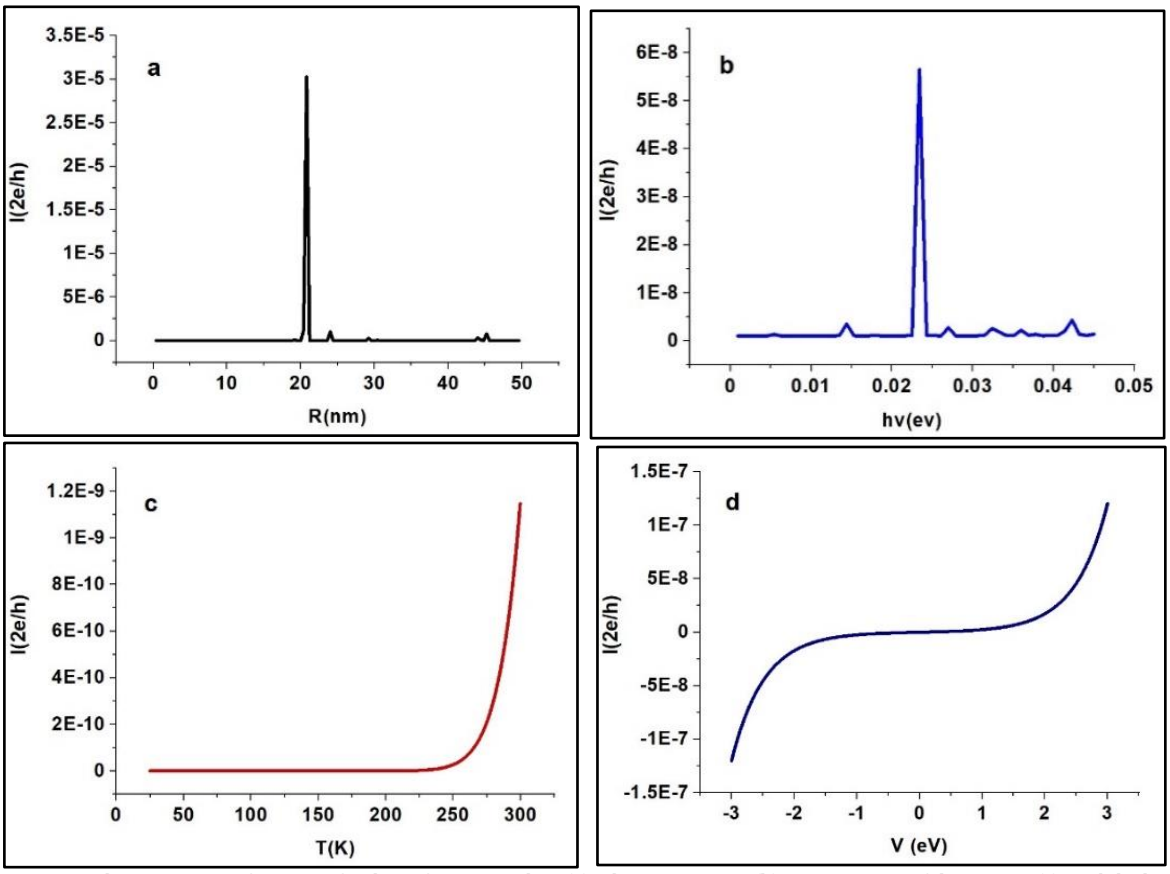

Figure 4. The current as a function of radius of quantum dots (a), photon energies (b), temperature of the system (c), and the bias voltage (d).

Conductance Results

Using the previous transmission calculations, the conductance calculations of the system can be obtained as was previously mentioned in equation (28). As shown in Fig. 5, the conductance characteristic was studied by observing the

correlation between the conductance values and QD radius R, E_{ph} and T. Fig. 5a illustrates the relationship between the conductance and R in which the conductance was raised suddenly at determined values of R and remained close to zero at another values. This can be due to the electron transfer process from HOMO level to LUMO level because of the photon effect. This electron transfer to LUMO level contributed to the enhancement of the conductance. Also, the conductance-E_{ph} correlation is shown in Fig. 5b in which the conductance was enhanced with the increment of the incident photon energy. This enhancement began to be oscillated near determined value when reach a limit value of energy of incident photon. Further, in this conductance calculations with respect to T, it was considered that the system is in the thermal equilibrium in which $T_R=T_L=T$ with $0 < T < 300$ K as shown in Fig. 5c. It is clearly observed that the conductance is independent of temperature in the range of $0 < T < 225$K in which the conductance is not affected by the increment of temperature. However, when T reaches nearly 225K and above, a nonlinear relation was observed in which there is a high and sudden increment in the conductance with normal raising of temperature. This may be attributed to the thermal broadening of the Fermi function and the effects of molecular vibrations which is not included in our treatment.

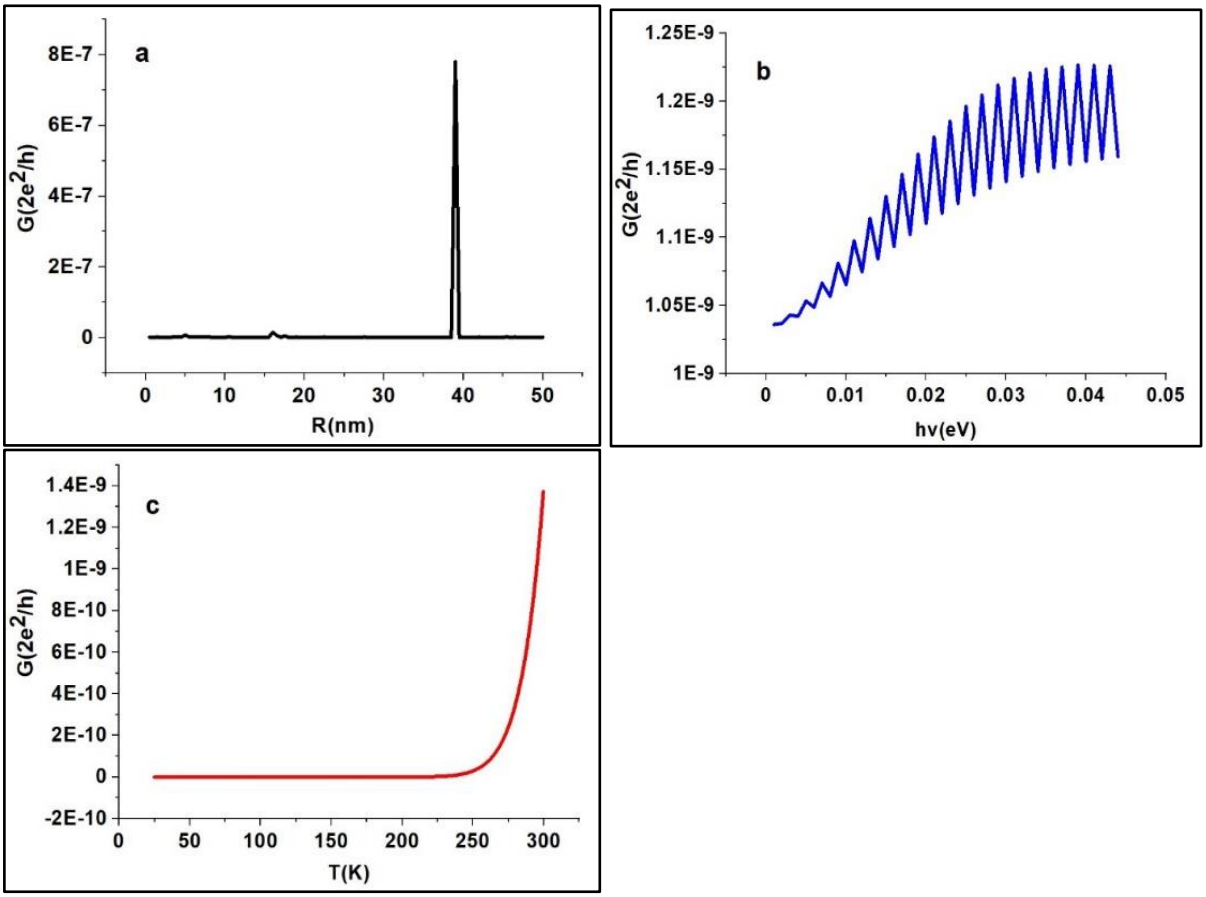

Figure 5. The conductance as function of radius of quantum dots (a), photon energies (b), temperature of the system (c).

Conclusion

In response to the research efforts devoted to developing and finding out new techniques and systems that interduce new concepts in producing low-cost devices with high performance, nano-dimension building block materials have been introduced to fill this need. Among these systems, DQDs structures can be used to fabrication optoelectronic devices with low cost and high performance due to their unique properties. Therefore, in this work, optoelectronic characteristics of QDs have been studied considering the quantum confinement effect of the semiconductor materials. This refers to the size-dependence of the semiconductor and band gap-

energy in nano crystals smaller than Bohr excitation radius which have quantized energy levels. We have presented the possibilities of designing nano optoelectronic device by using DQDs structure and adopting the central idea of arrangement QDs geometric due to the unique characteristics of this system in response to incident light. The proposed DQDs system consist of QDs placed on top of each other, connected parallelly and have size symmetry with different gap energies. A tight-binding model was used to illustrate the model and all the calculations were carried out using the steady state formalism. Transmission, current and conductance results of the suggested system were presented and discussed. An obvious correlation of the presented optoelectrical properties of the system with QD radius R, incident photon energy E_{ph}, Temperature and bias voltage have been found. Thus, the proposed structure analysis can be very sensitive to these parameters and would be considered as potential candidate for designing nano scale solar cell. Thus, DQDs system can be embedded next in the structure of different layers of photoelectric devices to study the variation of their characteristics in response to incident light.

Acknowledgements

Authors would like to acknowledge Prof. Jenan Majeed AL-Mukh and Prof. Shakier Ibraheem Easa from Basrah University for their useful information and support. Also, authors would like to acknowledge the support of the University of Thi-Qar and the Iraqi Ministry of Higher Education and Scientific Research.

References

Al-Mebir AAK. *Effect of In Situ Thermal Annealing Process on Structural, Optical and Electrical Properties of CdS\CdTe Thin-Film Solar Cells Fabricated by Pulsed Laser Deposition* (Doctoral dissertation, University of Kansas) 2015.

Al-mebir AAK, Al-Saidi SA. Theoretical Investigation of Base Pairs-Dependent Electron Transport in DNA System. In *Journal of Physics: Conference Series*, 2020; 1530(1): 012147.

AL-Saidi SA, Al-mebir AAK. Asymmetric Double Quantum Dot Structure as Nanoscale Diode. *University of Thi-Qar Journal* 2018; 13(4): 1-17.

Al-Saidi SA, Al-mebir AAK. Electronic Properties Simulation of Guanine Molecule. *In Journal of Physics: Conference Series*. IOP Publishing 2020; 1530(1): 012148.

Alivisatos AP. Semiconductor clusters, nanocrystals, and quantum dots. *Science* 1996; 271(5251): 933-937.

Bradshaw LR, Knowles KE, McDowall S, Gamelin DR. Nanocrystals for luminescent solar concentrators. *Nano letters* 2015; 15(2): 1315-1323.

Brus LE. Electron–electron and electron-hole interactions in small semiconductor crystallites: The size dependence of the lowest excited electronic state. *The Journal of chemical physics* 1984; 80(9): 4403-4409.

Carey GH, Abdelhady AL, Ning Z, Thon SM, Bakr OM, Sargent EH. Colloidal quantum dot solar cells. *Chemical reviews* 2015; 115(23): 12732-12763.

Ciftja O. Understanding electronic systems in semiconductor quantum dots. *Physica Scripta* 2013; 88(5): 058302.

Cuniberti G, Maciá E, Rodriguez A, Römer RA. Tight-binding modeling of charge migration in DNA devices. *In Charge Migration in DNA* 2007: 1-20.

Currie MJ, Mapel JK, Heidel TD, Goffri S, Baldo MA. High-efficiency organic solar concentrators for photovoltaics. *science* 2008; 321(5886): 226-228.

Dabbousi BO, Rodriguez-Viejo J, Mikulec FV, Heine JR, Mattoussi H, Ober R, Bawendi MG. (CdSe) ZnS core– shell quantum dots: synthesis and characterization of a size series of highly luminescent nanocrystallites. *The Journal of Physical Chemistry B* 1997; 101(46): 9463-9475.

Galperin M, Ratner MA, Nitzan A. Inelastic electron tunneling spectroscopy in molecular junctions: Peaks and dips. *The Journal of chemical physics* 2004; 121(23): 11965-11979.

Ghosh Chaudhuri R, Paria S. Core/shell nanoparticles: classes, properties, synthesis mechanisms, characterization, and applications. *Chemical reviews* 2012; 112(4): 2373-2433.

H. Sargent, E. (2005). Infrared quantum dots. *Advanced Materials*, 17(5): 515-522.

Ito T, Okazaki S. Pushing the limits of lithography. *Nature* 2000; 406(6799): 1027-1031.

Jin J, Tu MWY, Zhang WM, Yan Y. Non-equilibrium quantum theory for nanodevices based on the Feynman–Vernon influence functional. *New Journal of Physics* 2010; 12(8): 083013.

Kamat PV. Quantum dot solar cells. Semiconductor nanocrystals as light harvesters. *The Journal of Physical Chemistry C* 2008; 112(48): 18737-18753.

Kingon AI, Maria JP, Streiffer S. Alternative dielectrics to silicon dioxide for memory and logic devices. *Nature,* 2000; 406(6799): 1032-1038.

Lhuillier E, Scarafagio M, Hease P, Nadal, B, Aubin, H, Xu, XZ, Dubertret B. Infrared photodetection based on colloidal quantum-dot films with high mobility and optical absorption up to THz. *Nano letters* 2016; 16(2): 1282-1286.

Li XQ, Yan Y. Electrical transport through individual DNA molecules. *Applied Physics Letters* 2001; 79(14): 2190-2192.

Lloyd S. Ultimate physical limits to computation. *Nature* 2000; 406(6799): 1047-1054.

Lodahl P. Quantum-dot based photonic quantum networks. *Quantum Science and Technology* 2017; 3(1): 013001.

Lv Z, Wang Y, Chen J, Wang J, Zhou Y, Han, ST. Semiconductor quantum dots for memories and neuromorphic computing systems. *Chemical reviews* 2020; 120(9): 3941-4006.

McDonald SA, Konstantatos G, Zhang S, Cyr PW, Klem EJ, Levina L, Sargent EH. Solution-processed PbS quantum dot infrared photodetectors and photovoltaics. *Nature materials* 2005; 4(2): 138-142.

Nozik AJ, Beard MC, Luther JM, Law M, Ellingson RJ, Johnson JC. Semiconductor quantum dots and quantum dot arrays and applications of multiple exciton generation to third-generation photovoltaic solar cells. *Chemical reviews* 2010; 110(11): 6873-6890.

Peter Y, Cardona M. *Fundamentals of semiconductors: physics and materials properties*: Springer Science & Business Media 2010.

Qiao K, Deng H, Yang X, Dong D, Li, M, Hu, L, Tang J. Spectra-selective PbS quantum dot infrared photodetectors. *Nanoscale* 2016; 8(13): 7137-7143.

Reshma V, Mohanan P. Quantum dots: Applications and safety consequences. *Journal of Luminescence* 2019; 205: 287-298.

Rudan M. *Physics of semiconductor devices*: Springer 2015.

Song WS, Yang H. Efficient white-light-emitting diodes fabricated from highly fluorescent copper indium sulfide core/shell quantum dots. *Chemistry of Materials* 2012; 24(10): 1961-1967.

Talapin DV, Lee JS, Kovalenko M, Shevchenko EV. Prospects of colloidal nanocrystals for electronic and optoelectronic applications. *Chemical reviews* 2010; 110(1): 389-458.

Walter MG, Warren EL, McKone JR, Boettcher SW, Mi Q, Santori EA, Lewis NS. Solar water splitting cells. *Chemical reviews* 2010; 110(11): 6446-6473.

Fabio RA, Caprì T, Buzzai C, Pittalà V, Gangemi A. Auditory and visual oddball paradigm evaluated through p300 in five girls with rett syndrome. *NeuroQuantology* 2019; 17(7): 40-49.

Gaiseanu, F. Human/humanity, consciousness and universe: Informational relation. *NeuroQuantology* 2019; 17(5): 60-70.